Journal of Applied Sciences

ISSN 1812-5654

science alert

ANSInet
an open access publisher
http://ansinet.com

Journal of Applied Sciences 11 (1): 66-75, 2011
ISSN 1812-5654 / DOI: 10.3923/jas.2011.66.75

H_infinity Controller Design to Control the Single Axis Magnetic Levitation System with Parametric Uncertainty

Basheer Noaman Hussein, Nasri Sulaiman, R.K. Raja Ahmad,
Mohammad Hamiruce Marhaban and Hazem I. Ali
Department of Electrical and Electronic Engineering,
Faculty of Engineering, University Putra Malaysia, Malaysia

Abstract: In this study the force control design of single axis magnetic levitation system using H_infinity controller is presented. First, the system dynamics are linearized and described in transfer function form. Second, the magnetic force is regulated using H_infinity controller to achieve robust stability, disturbance/noise rejection and asymptotic tracking. A multiplicative unstructured model extracted from the parametric uncertainty is used for H_infinity control design. The obtained results showed that robust stability and performance have been achieved. On the other hand, an improved and more reliable time response compared with previous work also has been achieved in this study.

Key words: Robust control, H_infinity control, uncertain systems, nonlinear systems, multiplicative uncertainty, magnetic levitation system

INTRODUCTION

The potential uses of magnetic levitation systems range from standstill applications which use light current, such as active magnetic bearings, vibrating tables, wafer conveyors, micro machines, etc., to the levitation and guidance of electrical vehicles which need high current. The magnetic levitation has no contact between the moving object and fixed part. It is one of the good tools for a micro-machine because mechanical friction disappears, which increases the resolution and accuracy of the positioning device. Another advantage of the magnetic levitation system is that the manipulator can operate as a rigid body rather than using jointed parts such as robots, which means that position errors do not compound and the dynamic behavior is simple to model. The major disadvantage of levitation is that the system is inherently unstable and hence feedback control is usually required for stabilization (Yi *et al*., 1996; Chao-Lin *et al*., 2005). Due to the features of the open-loop instability and highly inherent nonlinearities in electromechanical dynamics of the magnetic levitation systems, the development of a high performance control design for the position control of the levitated magnets is very important. Since, it is very difficult to acquire an exact mathematical model to describe the electromechanical dynamics of the magnetic levitation systems, in general, only the approximated dynamic model are used. Therefore, many studies have been reported and discussed based on the approximated dynamic models in the recent years (Ono *et al*., 2002; Chen *et al*., 2003; Kaloust *et al*., 2004; Grochmal and Lynch, 2007). Magnetic levitation systems have been successfully and widely implemented for many engineering applications, such as vibration isolation, frictionless bearings, high-speed maglev passenger trains and fast-tool servo systems (Chiang *et al*., 2006; El-Hajjaji and Ouladsine, 2001; Trumper *et al*., 1997; Hurley *et al*., 1997).

The development of magnetically levitated micro machines has been reported in the literature. Tsuda *et al*. (1987) have designed a Magnetically Supported Intelligent Hand (MSIH) which uses active DC-type magnetic bearings. Hollis *et al*. (1987) have designed a hexagonal shaped magnetically levitated wrist using permanent magnets and air-core electromagnets. Park *et al*. (1996) have designed a six degree-of-freedom high precision positioner employing an antagonistic property which is generated by using permanent magnets and air-core electromagnets. Using precise control, the above mechanisms can carry out various automatic assembly tasks like active/advanced Remote Center Compliance (RCC) device. Banerjee *et al*. (2007) have designed and implemented a single axis magnetic levitation system for the suspension of a platform by using cascade lead compensator designed using the classical synthesis method. An attemption has been done to examine various micro-machine technologies, including piezoelectric, hydraulic, magnetic, shape memory alloy,

Corresponding Author: Basheer Noaman Hussein, Department of Electrical and Electronic Engineering, Faculty of Engineering, University Putra Malaysia, Malaysia

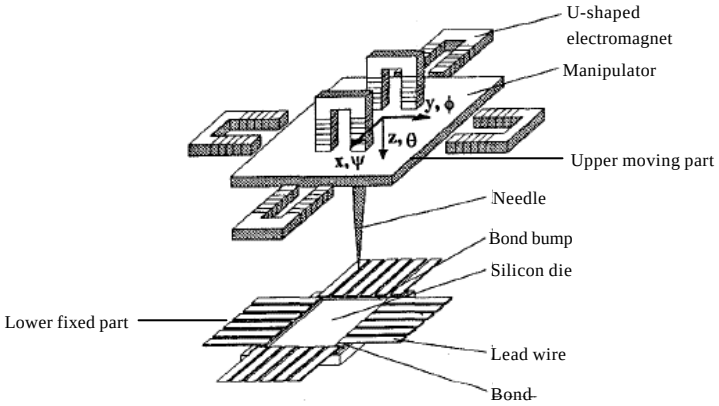

Fig. 1: Conceptual design for the shear force tester

and electrostatic approaches. Of particular note and the attempts to build electrostatic micro-motors using silicon-based technology (Trimmer and Gabriel, 1987; Bart *et al*., 1988; Tai *et al*., 1989). The motivations for using a silicon-based technology are the ability to have good process control and the potential savings in cost obtained with batch fabrication, particularly if the electronics are integrated with the mechanical devices (Busch-Vishniac *et al*., 1990).

In some applications, micro-machines require a strategy of force control. For example, in semiconductor fabrication, force control is needed for mechanical quality control testing for bonds between circuits on devices. One possible conceptual design in the field of Micro-machines is the shear force tester shown in Fig. 1. The tester consists of U-shaped electromagnets and a manipulator (a rectangular piece of metal), both are made of iron. It is assumed that the xyz coordinate system is fixed at the centre of the manipulator and ψ, ϕ and θ are the Eulerian angles of the xyz coordinate system. Due to the magnetic suspension, spring forces serve as stabilizing forces on the manipulator and, hence, making the manipulator stable in both ψ and ϕ directions and unstable in *è* direction. A known force can be applied to the bond in the z direction (Yi *et al*., 1996).

In this application, only one degree-of-freedom motion in the z direction will be examined, with the assumption that all other motions are stabilized. The force is determined from measurement of the flux density.

The goal of robust systems design is to retain assurance of system performance in the presence of model uncertainty. A system is robust when its performance performs adequately under model uncertainty. A control system is robust when (1) it has low sensitivity, (2) it is stable over the range of parameter

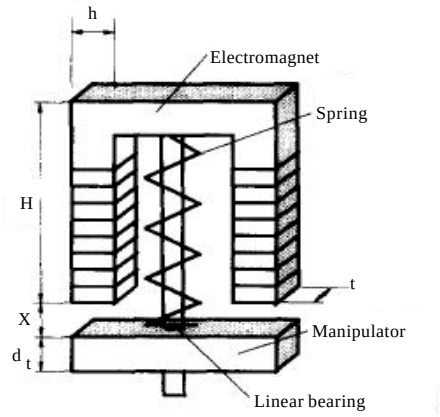

Fig. 2: A single axis magnetic levitation system

variations and (3) the performance continues to meet the specification in the presence of uncertainty (Ali *et al*., 2009).

H_infinity is one of the most known techniques available nowadays to design a robust control (It is an optimization method that takes into consideration a strong definition of the mathematical way to express the ability to include both classical and robust control concepts within a single design framework). With this method, model uncertainties and performance requirements can be incorporated into a single framework of H_infinity controller achieve very robust stability and good performance in theory (Zhou and Doyle, 1998).

System dynamics A single axis force controlled Magnetic Levitation System (MLS), shown in Fig. 2, is considered to derive a mathematical formulation of system motion. In addition to the electromagnet and the manipulator, a spring and a linear bearing are used for providing a reaction force and constraining the manipulator motion to

the vertical direction, respectively. The U-shaped iron core magnet can produce a strong magnetic force, which is a good advantage (Yi *et al*., 1996).

The fundamental equation of motion of the system is derived from Newton's second law of motion as:

$$m\ddot{z}(t) = \sum \text{forces} \quad (1)$$

Four physically different forces are acting on the manipulator mass. They are the gravitational force, the electromagnetic force (attraction or repulsion), the spring force and any possible internal or external disturbance. It is important to note here that the disturbance force is also introduced to compensate for any neglecting of specific physical modes, which may be considered in the mathematical formulation as will be shown below. Therefore, the equation of motion of the system is (Yi *et al*., 1996).

$$m\ddot{z}(t) = mg - f(t) - k_s(z(t) - z_n) + f_{dis}(t) \quad (2)$$

where, m is the manipulator mass, g is the gravity of earth (acceleration), z (t) is the air gap length, z_n is the air gap length when no spring force exists (assumed neglected), f (t) is the time function electromagnetic force, k_s is the spring constant and $f_{dis}(t)$ is a time function of disturbance force or model uncertainty.

Figure 3 shows the free body diagram of the single axis magnetic levitation system to describe all the forces that may have an effect.

The magnetic force can be expressed in terms of the flux density B by assuming the magnetic flux is uniform in the air gap and the permeability of iron is high enough to be considered. The equation of magnetic force f in terms of flux density is as follows:

$$f(t) = k_f B^2(t) \quad (3)$$

where, B is the flux density and k_f is expressed as:

$$k_f = \frac{A}{\mu_0} \quad (4)$$

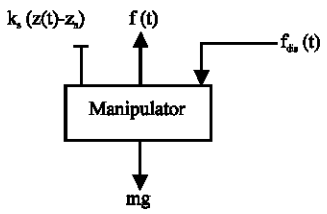

Fig. 3: Free body diagram of single axis magnetic levitation system

where, A is the magnetic pole face area and μ_0 is the permeability of free space.

The instantaneous flux density B(t) and, hence, the instantaneous electromagnetic force f (t) are produced by the electrical coil circuit. The equation relating the coil voltage e, flux density B and the air gap length z is expressed as (Theraja, 1984).

$$e(t) + e_{dis}(t) = NA\frac{dB(t)}{dt} + \frac{2R}{\mu_0 N}B(t)z(t) \quad (5)$$

where N is the number of coil turns, R is the coil resistance and e_{dis} is the voltage noise. Again this noise voltage is added not only to compensate for changes in the voltage source but also for any mathematical simplification that may be carried in Eq. 5.

Since the MLS consists of both electrical and mechanical elements, then the generalized Lagrange method of modelling can be used to obtain the complete mathematical modelling of the system.

Equations 2 and 5 represent the two basic differential equations of the considered MLS. These equations depict nonlinear elements, the square of flux density B^2 and the product Bz. Moreover, if one assumes that f_{dis} and/or e_{dis} are random quantities then the solution would not be found analytically. One way to solve the problem is to apply the theory of small perturbation around nominal steady state parameter values.

Let F_0, B_0, Z_0 and E_0 be the nominal values of the magnet force, flux density, air gap length and coil voltage, respectively and let δ_f, δ_B, δ_z, δ_e be the deviation of these quantities from the nominal values. To apply the theory of deviation to the time function variables, it yields:

$$f(t) = F_0 + \delta_f(t) \quad (6)$$

$$S(t) = F_0 + \delta_B(t) \quad (7)$$

$$S(t) = z_0 + \delta z(t) \quad (8)$$

$$e(t) = E_0 + \delta_e(t) \quad (9)$$

The nominal flux density can be measured by the following equation (Mohamed *et al*., 1994):

$$B_0 = \frac{0.5\mu_0 NE_0\sqrt{1 + \frac{2Z_0}{\pi h}}}{RZ_0} \quad (10)$$

Next, the independent variable (t) will be dropped for simplicity of writing. The magnetic force can be related to the flux density by substituting Eq. 6 and 7 in Eq. 3:

$$F_0 + \delta_f = k_f (B_0 + \delta^2_B) \quad (11)$$

$$F_0 + \delta_f = k_f (B^2_0 + 2B_0\delta_B + \delta^2_B) \quad (12)$$

$$F_0 + \delta_f = k_f B^2_0 + 2k_f B_0\delta_B + k_f\delta^2_B \quad (13)$$

By neglecting the second order term, which is valid if $|\delta_B| << |B_0|$, then

$$F_0 = k_f B^2_0 \quad (14)$$

$$\delta_f = 2k_f B_0\delta_B \quad (15)$$

The last two equations show that the force can be determined from flux density measurement. By substituting these two equations and Eq. 8 in 2, the system dynamics can be written as follows:

$$m(Z_0 + \delta_z) = mg - k_f B^2_0 - 2k_f B_0\delta_B - k_s(Z_0 + \delta_z) + f_{dis} \quad (16)$$

$$m\ddot{\delta}_z = mg - k_f B^2_0 - 2k_f B_0\delta_B + k_s\delta_z + f_{dis} \quad (17)$$

$$m\ddot{\delta}_z = -k_s\delta_z - 2k_f B_0\delta_B + f_d \quad (18)$$

where,

$$f_d = mg - k_f B^2_0 - k_s Z_0 + f_{dis} \quad (19)$$

On the other hand, after substituting equations in Eq. 5, it yields

$$NA\frac{d(B_0 + \delta_B)}{dt} + \frac{2R}{\mu_0 N}(B_0 + \delta_B)(Z_0 + \delta_z) = (E_0 + \delta_e) + e_{dis} \quad (20)$$

$$NA\frac{d + \delta_B}{dt} + \frac{2R}{\mu_0 N}(B_0 Z_0 + B_0\delta_z + \delta_B Z_0 + \delta_B\delta_z) = E_0 + \delta_e + e_{dis} \quad (21)$$

$$NA\dot{\delta}_B = \frac{2R}{\mu_0 N}B_0\delta_z - \frac{2R}{\mu_0 N}\delta_B Z_0 + \delta_e + e_d \quad (22)$$

where,

$$e_d = \frac{2R}{\mu_0 N}B_0 Z_0 + \frac{2R}{\mu_0 N}\delta_B\delta_z + E_0 + e_{dis} \quad (23)$$

Therefore, Eq. 18 and 22 represent a linear version of the original system equations and all nonlinear modes are put in the model uncertainties f_d and e_d.

There are three physical quantities in the system to be assigned as system states. They are the air gap length (z), the flux density (B) and the electric coil voltage (e). Let the system states be defined as follows:

$$x_1(t) = \delta_z(t) \quad (24)$$

$$x_2(t) = \dot{\delta}_z(t) \quad (25)$$

$$x_3(t) = \delta_B(t) \quad (26)$$

$$u(t) = \delta_e(t) \quad (27)$$

where u (t) is the system input signal.

By substituting Eq. 18 in Eq. 25 and 22 in 26 the state space representation of the system dynamics can be expressed as:

$$\dot{x}_1 = x_2 \quad (28)$$

$$\dot{x}_2 = -\frac{k_s x_1}{m} - \frac{2k_f B_0 x_3}{m} + \frac{f_d}{m} \quad (29)$$

$$\dot{x}_3 = -\frac{2RB_0 x_1}{\mu_0 N^2 A} - \frac{2RZ_0 x_3}{\mu_0 N^2 A} + \frac{\mu}{NA} + \frac{e_d}{NA} \quad (30)$$

The state variables can be arranged in a vector form as:

$$\dot{x}_p(t) = [x_1(t)x_2(t)x_3(t)]^T \quad (31)$$

$$\dot{x}_p(0) = [Z_0\,0\,B_0]^T \quad (32)$$

$$d(t) = [f_d e_d]^T \quad (33)$$

$$Y_f(t) = \delta_f(t) \quad (34)$$

Therefore, the dynamic model of the magnetic levitation system can be represented in a state space form as:

$$\dot{x}_p(t) = A_p x_p(t) + B_p u(t) + W_p d(t) \quad (35)$$

$$Y_f(t) C_p x_p(t) + n(t) \quad (36)$$

where, n (t) is the sensor noise (random disturbance), d (t) is the input disturbance that represents the model uncertainty and voltage noise signal and

$$A_p=\begin{bmatrix} 0 & 1 & 0 \\ -\frac{k_s}{m} & 0 & -\frac{2K_fB_0}{m} \\ -\frac{2RB_0}{\mu_0N^2A} & 0 & \frac{-2RZ_0}{\mu_0N^2A} \end{bmatrix} B_p=\begin{bmatrix} 0 \\ 0 \\ \frac{1}{NA} \end{bmatrix}$$

$$C_p=[0 \quad 0 \quad 2k_fB_0]\ W_p=\begin{bmatrix} 0 & 0 \\ \frac{1}{m} & 0 \\ 0 & \frac{1}{NA} \end{bmatrix} D=[0] \tag{37}$$

The system state space defined by Eq. 37 can be converted to a transfer function using:

$$G_p(s)=C(SI-A)^{-1}B+D \tag{38}$$

$$G_{d,n}(s)=C(SI-A)^{-1}W_p+D \tag{39}$$

And the following transfer functions can be obtained:

$$G_p(S)=\frac{b_2s^2+b_0}{s^3+a_2s^2+a_1s+a_0} \tag{40}$$

$$G_d(S)=\frac{b_1s}{s^3+a_2s^2+a_1s+a_0} \tag{41}$$

$$G_n(s)=\frac{b_2s^2+b_0}{s^3+a_2s^2+a_1s+a_0} \tag{42}$$

where,

$$b_2=(2k_fB_0)(\frac{1}{NA})$$

$$b_1=(\frac{4k^2{}_fB^2{}_0}{m^2})$$

$$b_0=\left(\frac{k_s}{m}\right)\left(2k_fB_0\right)\left(\frac{1}{NA}\right)$$

$$a_2=\left(\frac{2RZ_0}{\mu_0N^2A}\right) \tag{43}$$

The parameters for the system are listed in Table 1. The system dynamics can be described by linear control system as shown in Fig. 4.

The H_infinity synthesis has been used to design a force controller for the magnetic levitation system such that the following requirements are achieved: robust stability against various model uncertainties, disturbance/noise attenuation, asymptotic tracking to command signals, less control energy and limiting closed loop bandwidth to achieve good robustness and noise rejection (Zhou *et al*., 1998; Mohamed *et al*., 1994).

Table 1: The parameters of the magnetically levitated system

Parameter	Description	Value	Units
A	Pole face area	0.004	m^2
B_0	Nominal flux density	0.0687	Tesla
	Manipulator thickness	0.012	m
E_0	Nominal voltage	7.37	V
H	Electromagnet width	0.02	m
H	Electromagnet height	0.01	m
F_0	Nominal force	15.04	N
M	Manipulator mass	0.153	Kg
N	Coil Turns	410	Turns
R	Resistance	4.6	Ù
T	Pole thickness	0.02	m
k_f	Force constant	3187	$N/Tesla^2$
Z_0	Nominal air gap	0.006	m
z_n	Air gap with no spring force	0.006	m
μ_0	Permeability of free space	1.25	$\mu N\ A^{-2}$
k_s	Spring constant	2257	$N\ m^{-2}$

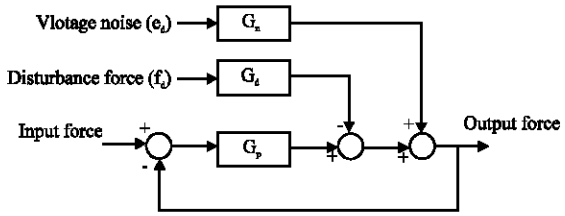

Fig. 4: Block diagram of the system

One of the important parts in the design of the H_infinity controller is the selection of weighting functions for specific design problems. This is not an easy procedure and often needs many iterations and fine-tuning and it is hard to find a general formula for the weighting functions that will work in every case (Anselmo and Moura, 1998). Therefore, to obtain a good control design, it is necessary to select suitable weighting functions. The performance and control weighting functions formula used in this work are (Zhou *et al*., 1998):

$$W_p(s)=\frac{K1*\left(\frac{s}{\sqrt{M_s}}+w_b\right)^2}{(s+W_b\sqrt{Ess})^2} \tag{44}$$

$$W_u(s)=\frac{K2*\left(s+\frac{w_{bc}}{\sqrt{M_u}}\right)^2}{(\sqrt{E_{ss}}s+W_{bc})^2} \tag{45}$$

where w_b is the minimum acceptable bandwidth (for disturbance rejection), M_s is the maximum peak magnitude of $|s(jw)|$, E_{ss} is the steady state error (allowed), K1 and

K2 are gains of the weighting functions, w_{bc} is the controller bandwidth and Mu is the magnitude of $h_\infty s$.

The weighting functions parameters are selected by trial and error to be w_b = 360, M_s = 1.5, E_{ss} = 0.0001, K1 = 0.1, K2 = 0.00008, w_{bc} = 150 and M_u = 10.

The H_∞ control design deals with both structured and unstructured uncertainty. However, since a design scheme involving unstructured uncertainty gives more control over the system (as it can cover not modelled dynamics at high frequencies (Nudehi and Farooq, 2007), the plant with structured uncertainty can be expressed in terms of unstructured multiplicative uncertainty. By selecting a set of nominal plants to evaluate the disk of uncertainty, the uncertainty plant is:

$$\hat{G}_p = G_p(1 + W_T\Delta_m) \tag{46}$$

where G_p is the nominal plant and the multiplicative uncertainty Δ can be expressed as:

$$\Delta_m = \frac{\hat{G}_p - G_p}{G_p} \tag{47}$$

The uncertain parameters of the system are R and m, which vary from 2 to 7Ω and 0.100 to 0.300 kg, respectively.

From Eq. 47, multiplicative uncertainty weight W_T can be calculated using curve fitting commands in MATLAB such that $|\Delta_m(jw)| \leq 1$ and can be expressed as:

$$w_T = \frac{0.03595s^2 + 32.8s + 8291}{s^2 + 62.82s + 3.379*10^4} \tag{48}$$

The H_∞ controller has been designed so that the infinity norm from input

$$w = \begin{bmatrix} R \\ f_d \\ e_d \end{bmatrix}$$

to output

$$z = \begin{bmatrix} e_f \\ u_f \end{bmatrix}$$

is minimized. Where w represents all exogenous input signals such as command signals (R), voltage noise (e_d) and disturbances (f_d); e_f, u_f are the weighted error and weighted control signals; u represents the actuator input; e is the error signal. Figure 5 shows the standard feedback diagram of the system with weights. The generalized plant P is expressed by:

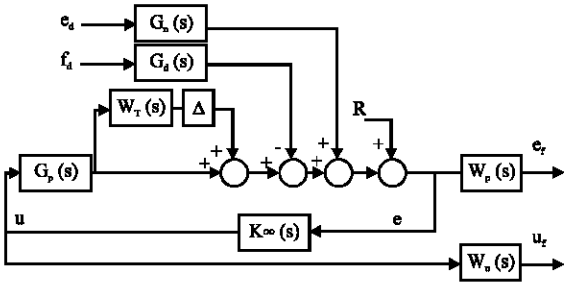

Fig. 5: Overall block diagram of the system

$$P = \begin{bmatrix} 0 & 0 & 0 & 0 & W_T G_p \\ -W_p & W_p & W_p G_d & -W_p G_n & -W_p G_p \\ 0 & 0 & 0 & 0 & W_u \\ -1 & 1 & G_d & -G_n & -G_p \end{bmatrix} \tag{49}$$

The lower linear fractional transformation of the generalized plant P and controller K_∞ can be described by:

$$F_l(P, K_\infty) = P_{11} + P_{12}K_\infty(1 - P_{22}K_\infty)^{-1}P_{21} = N \tag{50}$$

$$N = \begin{bmatrix} -W_T T & WTT & W_T G_d T & -W_T G_n T \\ -W_p S & W_p S & W_p G_d S & -W_p G_n S \\ -W_u KS & W_u KS & W_u G_D KS & -W_u G_n KS \end{bmatrix} \tag{51}$$

where, S is the sensitivity function of the nominal plant and T is the complementary sensitivity function, they can be defined as (Zhou *et al*., 1998):

$$S(s) = \frac{1}{1 + G_p(s)K_\infty(s)} \tag{52}$$

$$T(s) = \frac{G_p(s)k_\infty(s)}{1 + G_p(s)K_\infty(s)} \tag{53}$$

The design goal is to find the controller I that internally stabilizes the system such that the maximum singular value of N is minimized.

In order to achieve robust stability, less control energy and robust performance, the following constraints must be achieved:

$$\left\| \begin{matrix} S(s)W_p(s) \\ KS(s)Wu(s) \\ T(s)WT(s) \end{matrix} \right\| \leq 1 \tag{54}$$

The H_infinity controller is obtained by using the H_infinity robust controller command (hinf) in MATLAB. After some iteration the H_infinity controller which achieves the robustness and performance goals was found to be:

$$K_{\infty}=\frac{2.5*10^{7}{}_{8}^{6}+2.4*10^{11}{}_{8}^{5}+6.1*10^{14}{}_{8}^{4}+1*10^{17}{}_{8}^{8}}{{}_{8}^{7}+2.2*10^{6}{}_{8}^{6}+8*10^{9}{}_{8}^{5}-2.5*10^{18}{}_{8}^{4}-1.2*10^{17}{}_{8}^{8}}\\ \frac{+1.6*10^{19}{}_{8}^{2}+7.6*10^{20}{}_{8}+9.6*10^{21}}{-1.1*10^{17}8^{2}+4.3*10^{19}{}_{8}+3.3*10^{20}} \quad (55)$$

SIMULATION RESULTS

Figure 6a and b show the system output response characteristics. It is clear that the system becomes unstable when (a) a disturbance of 0.1 N step or (b) noise signals of 0.1 N step are applied. One of the important achievements of applying ✿ controller is to ensure the robust stability of the system. Figure 7 shows the frequency characteristics of the sensitivity function compared with the inverse of the performance weighting function. It is clear that the first performance criterion in Eq. 54 has been satisfied that means the sensitivity function is always less than the inverse of the performance weighting function w_p . The second performance criterion in Eq. 54 also has been achieved as shown in Fig. 8 that means K (s) S (s) is always less than the inverse of the performance weighting function w_p. Figure 9 shows the frequency characteristics of the complementary sensitivity function compared with the inverse of the multiplicative uncertainty weighting function. It is clear that the third performance criterion in Eq. 54 has been satisfied that means the complementary sensitivity function is always less than the inverse of the multiplicative uncertainty weighting function w_T. Figure 10 shows the frequency response of the controlled system

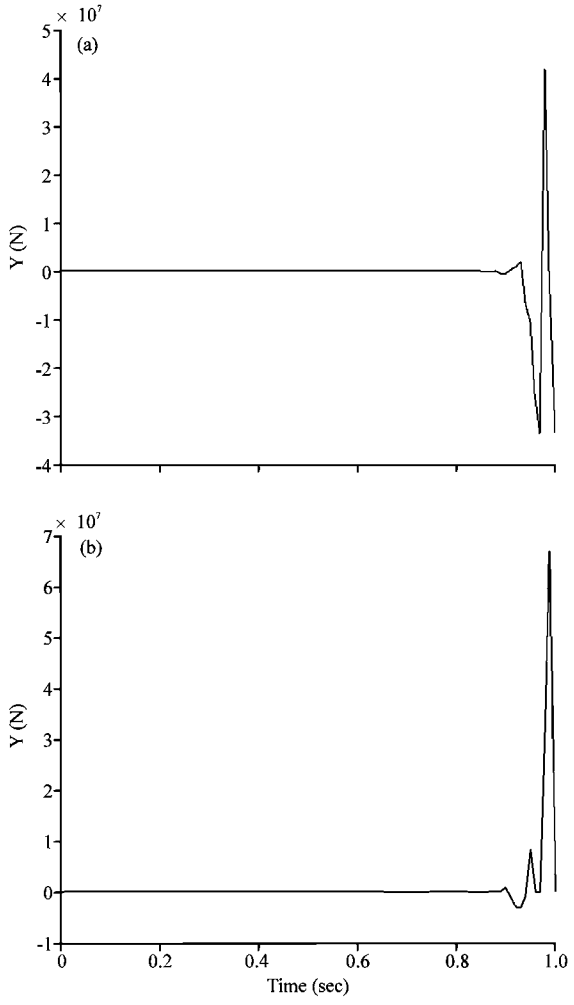

Fig. 6: The system output response for a 0.1 N step input (a) with 0.1 N step disturbance force applied without H_infinity controller and (b) with 0.1 N step voltage noise applied without H_infinity controller

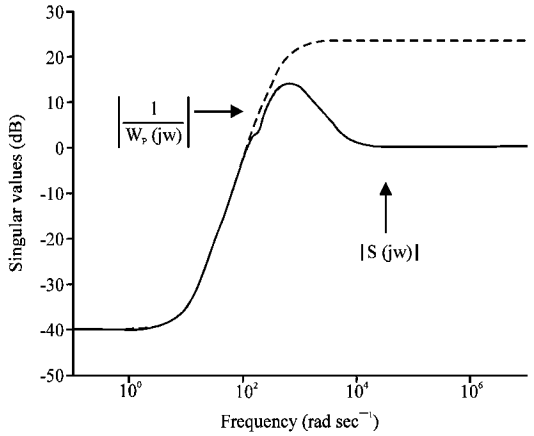

Fig. 7: The frequency response characteristics of the sensitivity function S(s) compared with the inverse of the performance weighting function Wp

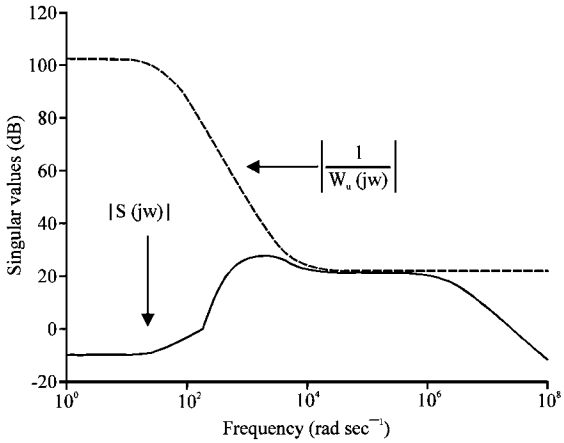

Fig. 8: The frequency response characteristics of the KS (s) compared with the inverse of the weighting function W_P

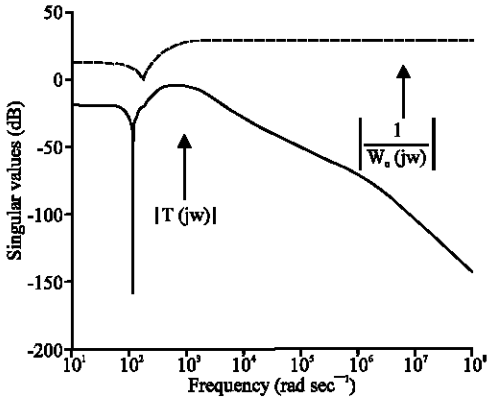

Fig. 9: The frequency response characteristics of the complementary sensitivity function T(s) compared with the inverse of the weighting function Wt

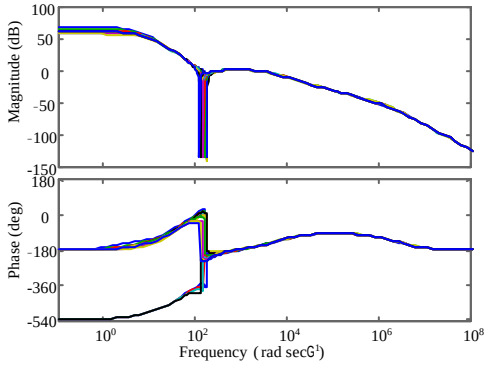

Fig. 10: The frequency response characteristics of the system with the controller

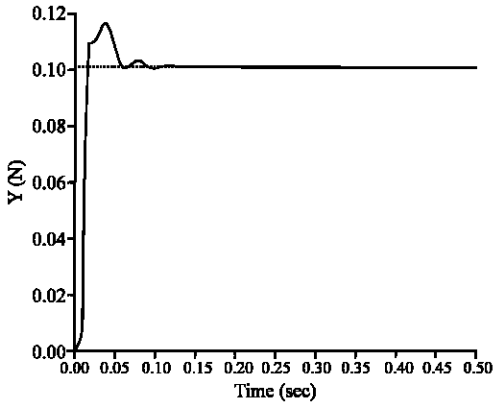

Fig. 11: The system output response for a 0.1 N step input with the controller

with all parameters uncertainty. It is shown that the system is stable with all parameters uncertainty; this means the robust stability of the system has been achieved. Figure 11 and 12 show the step response

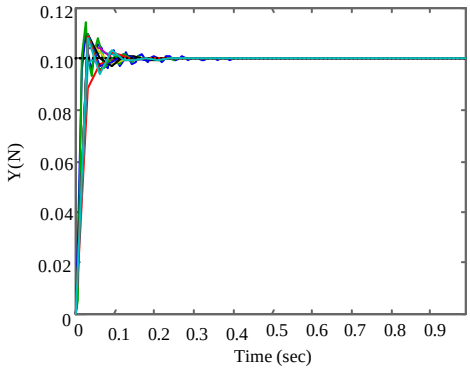

Fig. 12: The uncertain system output response for a 0.1 N step input with the controller

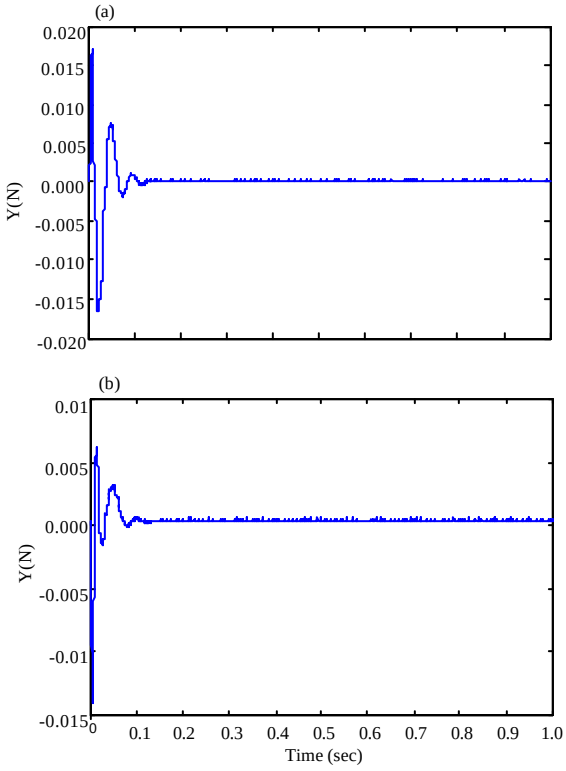

Fig. 13: The system output response for (a) 0.1 N step disturbance force with the controller and (b) for 0.1 N step voltage noise with the controller

characteristics of the nominal system and uncertain system. Figure 13a and b show the time response of the system when (a) a disturbance of 0.1 N step or (b) noise signals of 0.1 N step are applied respectively. It can be seen that a settling time of 0.1 sec has been achieved. An improved response has been obtained in comparison with results obtained from previous work. The obtained time

Table 2: Time response specifications of the controller

Specification	sec	sec	%	
Pole placement and controller (Previous work)	0.1	0.25	___	0.006
Controller	0.017	0.1	17%	0

response specifications are better in term of speed and error steady state than those obtained by previous theoretical and experimental work (Yi *et al*., 1996) as shown in Table 2.

CONCLUSION

A robust H_infinity controller for a single axis magnetic levitation system with model uncertainty has been presented. First the linear mathematical model of the system was derived. The unmodelled dynamic was taken into account as a disturbance to design the controller. Also the parameters uncertainty was considered. Adjusting the performance of the simulated closed loop response carried out the selection of the weighting functions. The appropriate selection of the weighting functions led to obtain a robust controller that achieves the force control in magnetic levitation system. Finally, the objectives of the controller were verified by simulation. An improved time response compared with previous work has been achieved.

REFERENCES

Ali, H.I., S.B.M. Noor, S.M. Bashi and M.H. Marhaban, 2009. Robust controller design for positioning a pneumatic servo actuator. Proceedings of the 2nd International Conference on Control, Instrumentation and Mechatronic Engineering, June 2-3, Malacca, Malaysia, pp: 36-42.

Anselmo, B. and S.R. Moura, 1998. z and i control for maglev vehicles. IEEE Control Syst., 18: 18-25.

Banerjee, S., D. Prasad and J. Pal, 2007. Design, implementation and testing of a single axis levitation system for the suspension of a platform. ISA Trans., 46: 239-246.

Bart, S.T., T.A. Lober, R.T. Howe, J.H. Lang and M.F. Schlecht, 1988.. Design considerations for micromachined electric actuators. Sensors Actuators, 14: 269-292.

Busch-Vishniac, I.J., S.J. Chen, M.C. Jeong, S.H. Li and I.Y. Wang, 1990. Magnetic levitation-based micro-automation of the mechanical process in semiconductor fabrication. Proceedings of the IEEE Investigation of Micro Structures, Sensors, Actuators, Machines and Robots, Feb. 11-14, Napa Valley, CA., pp: 142-146.

Chao-Lin, K., T.H.S. Li and N.R. Guo, 2005. Design of a novel fuzzy sliding-mode control for magnetic ball levitation system. J. Intel. Robotic Syst., 42: 295-316.

Chen, M.Y., M.J. Wang and L.C. Fu, 2003. A novel dual-axis repulsive maglev guiding system with permanent magnet: Modeling and controller design. IEEE/ASME Trans. Mechtrinacs, 8: 77-86.

Chiang, H.K., C.A. Chen and M.Y. Li, 2006. Integral variable-structure grey control for magnetic levitation system. IEE Proc. Electr. Power Appl., 153: 809-814.

El-Hajjaji, A. and M. Ouladsine, 2001. Modeling and nonlinear control of magnetic levitation systems. IEEE Trans. Ind. Elect., 48: 831-838.

Grochmal, T.R. and A.F. Lynch, 2007. Precision tracking of a rotating shaft with magnetic bearings by nonlinear decoupled disturbance observers. IEEE Trans. Control Syst. Technol., 15: 1112-1121.

Hollis, R.L., A.P. Allan and S. Salcudean, 1987. A six degree-of-freedom magnetically levitated variable compliance fine motion wrist. IEEE Trans. Robotics Automation, 7: 320-332.

Hurley, W.G. and W.H. Wolfle, 1997. Electromagnetic design of a magnetic suspension system. IEEE Trans. Educ., 40: 124-130.

Kaloust, J., C. Ham, J. Siehling, E. Jongekryg and Q. Han, 2004. Nonlinear robust control design for levitation and propulsion of a maglev system. IEE Proc. Control Theory Appl., 151: 460-464.

Mohamed, A.M., B. Vestgard and I. Busch-Vishniac, 1994. Real time implementation of a robust H8 controller for a 2-DOF magnetic micro-levitation positioner. Proc. Am. Control Conf., 1: 3219-3223.

Nudehi, S.S. and U. Farooq, 2007. Hybrid QFT/ for control of nonlinear systems: AN example of position control of a pendulum. Proc. Am. Control Conf., 1: 2793-2798.

Ono, M., S. Koga and H. Ohtsuki, 2002. Japan's superconducting Maglev train. IEEE Instru. Measure. Magazine, 5: 9-15.

Park, K.H., K.B. Choi, S.H. Kim and Y.K. Kwak, 1996. Magnetically levitated high precision positioning system based on antagoristic mechanism. IEEE Trans. Magneticsm, 32: 208-219.

Tai, Y.C., L.S. Fan and R.S. Muller, 1989. IC-processed micro-motors: Design, technology and testing. Proc. IEEE Micro Electro Mech. Syst., 1: 1-6.

Theraja, B.L., 1984. A Text Book of Electrical Technology. Division of Nirja Construction and Development Co. Ltd., Ram Nagar, New Delhi.

Trimmer, W.S.N. and K.J. Gabriel, 1987. Design considerations for a practical machined electrostatic micro motor. Sensors Actuators, 11: 189-206.

Trumper, D.L., M. Olson and P.K. Subrahmanyan, 1997. Linearizing control of magnetic suspension systems. IEEE Trans. Control Syst., 5: 427-438.

Tsuda, M., T. Higuchi and S. Fujwara, 1987. Magnetic supported intelligence hand for automated precise assembly. Proc. Conf. Ind. Elect. Control Instru., 80: 926-933.

Yi, J.H., K.H. Park, S.H. Kim, Y.K. Kwak, M. Abdelfatah and I. Busch-Vishniac, 1996. Robust force control for magnetic levitation manipulator using flux density measurement. Control Eng. Practic., 4: 957-965.

Zhou, K. and J.C. Doyle, 1998. Essentials of Robust Control. Prentice Hall, New York.